A Multi-criteria Design Optimization Framework for Haptic Interfaces

Ramazan Unal* Gullu Kiziltas† Volkan Patoglu‡

Faculty of Engineering and Natural Sciences
Sabancı University, İstanbul, Turkey

Abstract

This paper presents a general framework for optimization of haptic interfaces, in particular for haptic interfaces with closed kinematic chains, with respect to multiple design objectives, namely kinematic and dynamic criteria. Both performance measures are discussed and optimization problems for a haptic interface with best worst-case kinematic and dynamic performance are formulated. Non-convex single objective optimization problems are solved with a branch-and-bound type (modified culling) algorithm. Pareto methods characterizing the trade-off between multiple design criteria are advocated for multi-criteria optimization over widely used scalarization approaches and Normal Boundary Intersection method is applied to efficiently obtain the Pareto-front hyper-surface. The framework is applied to a sample parallel mechanism (five-bar mechanism) and the results are compared with the results of previously published methods in the literature. Finally, dimensional synthesis of a high performance haptic interface utilizing its Pareto-front curve is demonstrated.

Keywords: Multi-criteria design optimization, dimensional synthesis of parallel mechanisms, optimal design of haptic interfaces, kinematic and dynamic performance of manipulators.

Index Terms: B.8.2 [Hardware]: Performance and Reliability—Performance Analysis and Design Aids; C.4 [Performance of Systems]: Design studies; H.1.2 [Models and Principles]: User/Machine Systems; H.5.2 [Information Interfaces and Presentation]: User Interfaces—Haptic I/O; J.6 [Computer-Aided Engineering]: Computer-aided design.

1 Introduction

A *haptic interface* is a computer-controlled motorized device that physically interacts with a human operator to render presence of computationally mediated environments. An ideal haptic device is desired to withstand human applied forces with very high stiffness and be capable of displaying a full range of impedances down to the minimum value human can perceive. The performance of a haptic interface under closed loop control is measured by the *transparency* of the display, that is, by quantifying the match between the desired and actually rendered impedance values. During haptic rendering, the haptic interface is coupled to the control system and its existence results in parasitic effects on the displayed impedances, deteriorating the perfect transparency. Therefore, independent of the control algorithm used, both the kinematic and dynamic performance of the haptic device have an impact on the overall performance of the haptic display.

Robotic manipulators with parallel kinematic chains are popular among haptic interfaces due to their inherent advantages in satisfying requirements of haptic applications with respect to their serial counterparts. Parallel mechanisms offer compact designs with high stiffness and have low effective inertia since their actuators can be grounded in many cases. In terms of dynamic performance, high position and force bandwidths are achievable with parallel mechanisms thanks to their light but stiff structure. Besides, parallel mechanisms do not superimpose position errors at joints, hence can achieve high precision.

Despite these favorable characteristics of parallel mechanisms, optimal design of such mechanisms with closed kinematic chains is significantly more challenging. Parallel mechanisms have smaller workspace with possible singularities within the workspace and their analysis is considerably harder than the analysis of manipulators with serial kinematic chains. Due to the additional complexities involved, the dimensional synthesis of parallel mechanisms is still an active area of research.

Optimum design of parallel mechanisms even for a single objective function is challenging due to the nonlinear, large scale nature of such mechanisms [19] and non-convex properties of performance indices with respect to the design variables [26]. Many different optimization approaches applicable to nonlinear, non-convex optimization problems such as genetic algorithms [18, 19, 33, 38], simulated annealing [28], Bayesian techniques [33, 34], Monte-Carlo simulations [33, 38], controlled randomized searches [22], performance charts [20], workspace atlases [21], and branch and bound methods [31] have been applied to design optimization of parallel mechanisms. In general, deterministic methods can get stuck at a local optimum, heuristic methods cannot guarantee optimality of the converged solution, while branch and bound type methods are only as accurate as the discretization selected.

While designing the geometry of a haptic interface, various performance criteria such as kinematic and dynamic isotropy, singularity-free workspace, sensitivity, and transmission capability have to be considered *simultaneously*. The performance with respect to any of these criteria cannot be improved without deteriorating another; hence, design trade-offs are inevitable. Determination of optimal dimensions with respect to many design criteria is a difficult problem and should be handled with multi-objective optimization methods so that trade-offs can be assigned in a systematic manner.

As emphasized earlier, an optimal design of a haptic interface can only be achieved by considering many competing objectives. There exists several studies in which multiple design criteria have been addressed for this purpose. Hayward *et al.* define the relationship between multiple criteria and utilize sensitivities of these criteria to conduct a hierarchical optimization study [11]. Multiple objectives are considered sequentially in [1, 15, 28, 31] by searching for parameter sets resulting in near optimal kinematic performance and then selecting the design exhibiting the best dynamic performance from this reduced parameter space. Task-priority [3], probabilistic weighting [24], composite index [18], and tabular methods [35] are among the other approaches that consider multiple criteria.

Even though these studies can account for multiple design criteria, they can be broadly classified under *scalarization methods* in which the multi-criteria optimization problem is addressed in an indirect manner, by first transforming it into a (or a series of) single objective (scalar) problem(s). These approaches either aggregate multiple criteria into a single objective function through some form

*e-mail: ramazanunal@su.sabanciuniv.edu
†e-mail: gkiziltas@sabanciuniv.edu
‡e-mail: vpatoglu@sabanciuniv.edu

of weighting or prioritize one objective and select others to serve as constraints to form a single objective optimization model. Scalarization methods possess the inherent disadvantage of their aggregate objective functions requiring preferences or weights to be determined apriori, *ie.* before the results of the optimization process are actually known [6]. Since assigning proper weights or prioritizing different criteria is a problem dependent, non-trivial task, these techniques fall short of providing a general framework to the design of the parallel mechanisms.

Pareto methods, on the other hand, incorporate all optimization criteria within the optimization process and address them simultaneously to find a set of efficient solutions. Each design alternative in the solution set corresponds to a non-dominated design in the objective space. In other words, these methods aim to construct the Pareto-front hyper-surface representing the design trade-offs between multiple criteria. Once such a hyper-surface resolving the design trade-offs is obtained, an appropriate design on this hyper-surface can be selected taking into account other design requirements of the particular application in consideration. Pareto methods allow the designer to make an informed decision by studying a wide range of options, since they contain the solutions that are optimum from an *overall* standpoint; unlike aggregate optimization techniques that may ignore this trade-off viewpoint. Thanks to this feature, Pareto methods are better suited as a general solution framework for design optimization of parallel mechanisms, since they provide a better understanding of optimization problem allowing all the consequences of a decision with respect to all the objectives be explored.

As regards to employing Pareto methods for design of parallel mechanisms, Krefft *et al.* recently applied a modified genetic algorithm (GA) to the problem for multiple objective functions, solving for the Patero-front hyper-surface [17, 16]. Similarly in [30] GA is applied to multi criteria optimization of a 2-DoF parallel robot. Despite their inherent advantage of resulting in multiple non-dominated design solutions within a single optimization search, GA approaches suffer from several disadvantages. Specifically, the convergence performance of GA is highly dependent on user-specified parameters such as sharing factor, and the results are very sensitive to these user specified parameters. Moreover, GA methods demand inferior computational cost with increasing number of objective functions, hence cannot be easily adopted or scaled for use of more than two objective functions [4]. More importantly, GA might prematurely converge to sub-optimal solutions [12]. Finally, use of GAs to obtain Pareto front hyper-surface has the disadvantages of large computational expense as well as a tendency for clumping of solutions in objective space resulting in under-represented regions of the Pareto front [6].

In this paper, a multi-objective design framework for optimization of parallel mechanisms is presented. Global kinematic and dynamic performance of parallel mechanisms over a pre-defined singularity free workspace are maximized simultaneously and the Pareto-front curve for these two criteria is obtained. Firstly, the global solutions of non-convex min-max performance criteria are solved independently from each other using a modified branch and bound algorithm, called culling algorithm [31]. Once optimal solutions of each single criteria optimization problem are obtained, Normal Boundary Intersection (NBI) method [5], which performs a deterministic geometric search within the objective space, is utilized to efficiently compute uniformly distributed design solutions on the Pareto-front curve. The proposed framework is applicable to other performance indices and is easily extendable to include further design criteria that may be required by the application.

The paper is organized as follows: Section 2 discusses several kinematic and dynamic performance measures while Section 3 introduces the sample mechanism used for the analysis, a 2-DoF parallel five-bar linkage. Section 4 formulates the multi-criteria optimization problem. Section 5 explains the optimization methods used to address the single and multi-criteria optimization problems and is followed by results and their discussion in Section 6. Section 7 presents conclusions and future work. Finally, kinematic and dynamic analyses of a five-bar linkage are detailed in the Appendix.

2 Measuring Kinematic and Dynamic Performance

As elaborated in the introduction, both kinematic and dynamic performance of parallel mechanisms are to be optimized to achieve haptic devices with low parasitic effects. To quantify performance, several design matrices, including Jacobian and mass matrices, are studied and to date, many scalar performance indices have been proposed. These indices either represent a distance to a singular configuration or quantify the directional independence (uniformity) of configuration dependent design matrices. Since singular values of a matrix provide a versatile metric to quantify its properties, most of the indices are derived as a function of these values.

To measure kinematic performance, properties of the Jacobian matrix (J) are studied thoroughly. Condition number, proposed by Salisbury and Craig [29], describing the worst-case behavior at a given configuration is one of the most commonly used kinematic performance measures. Given as the ratio of the minimum and maximum singular values of the Jacobian matrix, this measure locally characterizes directional isotropy for both force/motion transmission accuracy and actuator utilization of a manipulator. Another popular index, manipulability, measures the ease of arbitrarily changing the position and orientation of the end effector and is calculated by taking the product of singular values of the Jacobian matrix [37]. Sensitivity characterizes the precision of a manipulator by measuring the change in end-effector configuration with respect to small perturbations of joint angles and is given by the sum of absolute values of Jacobian matrix elements in a single row [9]. Finally, minimum singular value of the Jacobian matrix is also proposed as a kinematic performance measure [14] as a value quantifying the skewness of the velocity response.

All of the above mentioned indices are *local* measures of kinematic performance; therefore, are not constant over the entire workspace. Extensions of these indices have been proposed to characterize the performance of a manipulator over the entire workspace. Gosselin and Angeles proposed *global* condition indices based on integral of local kinematic performance measures over the workspace [8]. However, being average values, this indices fail to capture possible low performance configurations (near singular points) within the workspace. Moreover, integrating a local measure can be computationally expensive. Mean of the minimum singular value has also been proposed as global measure in order to characterize the path velocity of parallel robots [15]. Since mean values are not sufficient to guarantee homogeneity of performance, standard deviation of the minimum singular value has also been introduced as a measure in [15]. Other global indices include global payload index that measures the force transmission capability [25]. Finally, the global isotropy index ($\mathcal{GII}$), introduced in [31] by Stocco *et al.*, is a workspace inclusive worst-case kinematic performance measure that is intolerant of poor performance over the entire workspace. $\mathcal{GII}$ is calculated as the ratio of the minimum of smallest singular value and maximum of largest singular value of the Jacobian matrix over the workspace.

In this paper, a global performance index is chosen to quantify the kinematic isotropy of the five-bar mechanism since the objective of the design problem is to minimize the parasitic effects of the manipulator over the workspace. Even though any global index can be utilized within the framework presented, to allow comparisons with earlier published results $\mathcal{GII}$ is preferred. As a global worst case performance measure, maximizing $\mathcal{GII}$ corresponds to designing a mechanism with best worst-case kinematic performance. Moreover, an optimal $\mathcal{GII}$ results in a uniform Jacobian matrix for the sake of precision, while also increasing the efficiency of utilization

of the actuators. $\mathcal{GII}$ can be mathematically expressed as

$$\mathcal{GII} = min_{\gamma_0,\gamma_1 \in W} \frac{\underline{\sigma}(J(\boldsymbol{\alpha}, \boldsymbol{\gamma}_0))}{\overline{\sigma}(J(\boldsymbol{\alpha}, \boldsymbol{\gamma}_1))} \quad (1)$$

where J represents Jacobian of the manipulator, $\underline{\sigma}$ and $\overline{\sigma}$ are the minimum and maximum singular values of the Jacobian matrix, $\boldsymbol{\gamma_0}$ and $\boldsymbol{\gamma_1}$ are the configurations in the workspace that result in the extreme singular values, $\boldsymbol{\alpha}$ is the column matrix of design variables, and W represents the workspace.

Dynamic performance is measured in a similar manner to the kinematic performance, but this time properties of the mass matrix (M) capturing the relation between actuator force/torque and end-effector acceleration, are studied. The goal for improving dynamic performance is to minimize inertia effects that conflict with high acceleration demands. To characterize *local* dynamic performance Asada defined the effective inertia matrix expressing the homogeneity of the moment of inertia of the non-redundant manipulators and introduced the concept of generalized inertia ellipsoid [2]. Yoshikawa proposed a dynamic manipulability measure [36], which is an extension of manipulability concept and measures the degree of arbitrariness in changing end-effector accelerations. Dynamic manipulability is calculated as the product of singular values of JM^{-1} matrix. Angeles *et al.* defined the dynamical conditioning index which measures dynamical coupling and numerical stability of the generalized inertia matrix of manipulators [23]. Finally, swiftness, a measure to characterize the attitude of the manipulator to produce high end-effector accelarations, is proposed by Di Gregorio *et al.* which can also be applied to planar manipulators with non-homogeneous generalized coordinates [10].

Similar to the case of local kinematic performance indices, extensions to local dynamic indices have been proposed to characterize the performance of a manipulator over the entire workspace. Calculating the mean value and standard deviation of the local dynamic indices are among the most commonly used approaches to achieve a global dynamic performance index. A global dynamic index ($\mathcal{GDI}$) is introduced in [31] to quantify the global worst-case performance of a manipulator. $\mathcal{GDI}$ measures the largest effect of mass on the dynamic performance by calculating the maximum largest singular value over the workspace of the effective mass matrix at the end-effector and is computed as inverse of this maximum of largest singular value.

To be consistent with the metric chosen for the kinematic performance, the workspace inclusive best worst-case performance measure ($\mathcal{GDI}$) is used to quantify dynamic performance. As mentioned earlier, any dynamic index could be utilized in the framework introduced, but this decision also allows for comparisons with earlier published results. As a global worst-case performance measure, maximizing $\mathcal{GDI}$ results in reduced maximum largest singular value of the effective mass matrix, decreasing the inertial interference by the system. $\mathcal{GDI}$ can be mathematically expressed as

$$\mathcal{GDI} = min_{\gamma \in W} \frac{1}{1 + \overline{\sigma}(M(\boldsymbol{\alpha}, \boldsymbol{\beta}, \boldsymbol{\gamma}))} \quad (2)$$

where M represents effective mass matrix of the manipulator as seen at the end effector, $\overline{\sigma}$ is the maximum singular value of the effective mass matrix, $\boldsymbol{\gamma}$ is the configuration in the workspace that results in the maximum singular value, $\boldsymbol{\alpha}$ is the column matrix of design variables, and W represents the workspace.

In general, since entries of Jacobian and mass matrices may not be homogenous in units, proper normalization is necessary such that the measures defined on these matrices are meaningful. Among several approaches proposed in literature, normalization with a characteristic length [13, 15] or a nominal link length [18], and partitioning the matrices into translational and rotational parts [15, 19] are the most popular choices. Normalization is not necessary for the sample problem presented in this paper, as it possesses only a translational workspace.

3 Five-Bar Linkage

The optimization framework presented in this paper is applied to a 2-DoF five-bar parallel mechanism due its sufficient richness with relative simplicity allowing better interpretation of the optimization problem at hand. Moreover, scalarization/aggregrate methods have been applied to the multi-criteria optimization of this mechanism in the literature, rendering comparisons of different approaches possible. The methods discussed in this paper constitute a general framework for design optimization of parallel mechanisms and is by no means limited to the sample mechanism studied.

A five-bar mechanism can be characterized by lengths l_0, l_1 , l_2, l_3 and l_4 of its five links and three variables r, γ and ν defining the position and orientation of its workspace as shown in Figure 1. To quantify the orientation of each link, joint angles q_i ($i = 1..4$) measured from the x-axis are introduced. A five-bar mechanism with symmetric link lengths ($l_1 = l_4$, $l_2 = l_3$) and a symmetric workspace that is located parallel to the x and y-axes of the global coordinate system ($\gamma = \pi/2$, $\nu = \pi/2$) is selected in this study. Moreover, out of four possible assembly configurations, only the elbow-out posture, as depicted in Figure 1, is studied. Optimality of the above listed decisions in terms of both kinematic and dynamic performance have already been shown in the literature [31].

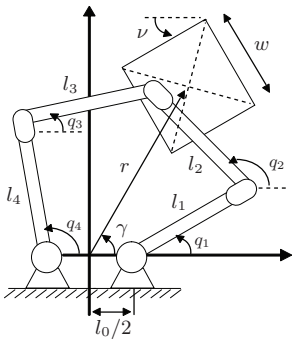

Figure 1: Five-bar mechanism in the elbow-out posture

Assuming that the dimension of the symmetric workspace w is pre-determined, the optimization problem can be formulated using four design variables: l_0, l_1, l_2 and r. Table 1 presents the design variables $\boldsymbol{\alpha}$ and design parameters $\boldsymbol{\beta}$ (parameters that do not change during the design process) for the symmetric five-bar mechanism.

Table 1: Design variables $\boldsymbol{\alpha}$ and parameters $\boldsymbol{\beta}$

	Symbol	Definition	Unit
α_1	l_0	Distance between actuated joints	mm
α_2	l_1, l_2	Length of actuated links	mm
α_3	l_2, l_3	Length of free links	mm
α_4	r	Workspace center position	mm
β_1	$w = 200$	Workspace side length	mm
β_2	$\gamma = 90^\circ$	Angle between r and x-axis	$^\circ$
β_3	$\nu = 90^\circ$	Angle between W and y-axis	$^\circ$

Kinematic and dynamic models of the symmetric parallel five-bar mechanism are detailed in the Appendix, along with the Jacobian and mass matrices to be used during the design optimization.

4 Optimization Problem

As discusses in Section 2, two objective functions characterizing the kinematic and dynamic performances of the mechanism are considered in this paper. The objective of optimization is to maximize the worst kinematic isotropy of the mechanism ($\mathcal{GII}$) while simultaneously minimizing the effective mass (max singular value of the effective mass matrix or $\mathcal{GDI}$). The negative null form of the

multi-objective optimization problem can be stated as

$$\begin{array}{c} max\ \mathbf{F}(\boldsymbol{\alpha},\boldsymbol{\beta},\boldsymbol{\gamma}) \\ \mathbf{G}(\boldsymbol{\alpha},\boldsymbol{\beta}) \leq 0 \\ \boldsymbol{\alpha}_a < \boldsymbol{\alpha} < \boldsymbol{\alpha}_u \end{array} \quad (3)$$

where $\mathbf{F}$ represents the column matrix of objective functions that depend on the design variables $\boldsymbol{\alpha}$, parameters $\boldsymbol{\beta}$, and workspace positions $\boldsymbol{\gamma}$. Symbol $\mathbf{G}$ represents the inequality constraint functions that also depend on design variables and parameters. Finally, $\boldsymbol{\alpha}_l$ and $\boldsymbol{\alpha}_u$ correspond to the lower and upper bounds of the design variables, respectively.

For the symmetric five-bar mechanism in elbow out posture, the column matrices $\mathbf{F}$ and $\mathbf{G}$ can be explicitly derived as

$$\mathbf{F} = \begin{bmatrix} \mathcal{GII} \\ \mathcal{GDI} \end{bmatrix}, \ \mathbf{G} = \begin{bmatrix} (l_0/2 + w/2)^2 + (r + w/2)^2 - (l_1 + l_2)^2 \\ -q_2 \\ q_2 - q_1 \end{bmatrix}$$

In these expressions, the first element of the $\mathbf{G}$ matrix constrains the design space to ensure a closed kinematic chain throughout the reachable workspace while last two elements stand for the elbow-out posture.

5 METHODS

In the previous section, the formulation for the multi-criteria optimization problem for best worst-case performance of a haptic interface is described. Before addressing the multi-criteria optimization problem, the nature of the problem with respect to the selected performance criteria is to be studied. Inspecting the performance criteria, one can conclude that both $\mathcal{GII}$ and $\mathcal{GDI}$ are non-convex with respect to the design variables. Moreover, as workspace inclusive measures, their calculation requires searches over the workspace. As discussed in the introduction, several methods have been proposed to solve for the single criteria optimization problem of parallel manipulators. In general, descent methods suffer from getting trapped at local optima while heuristic methods cannot guarantee optimality of their solution. Feasibility and efficiency of a branch-and-bound type method, called *culling algorithm*, is advocated in the literature to address single objective min-max problems [31].

In this study, a modified version of the culling algorithm is used to independently solve for the optimum designs with respect to $\mathcal{GII}$ and $\mathcal{GDI}$. The culling algorithm improves the computational efficiency of a brute-force method by reducing (culling) the amount of searches required through effective performance comparisons. The algorithm capitalizes on the fact that as a worst-case measure, once the global performance index for certain reference parameters is calculated conducting a search over the entire workspace, reduction of the feasible parameter set can be performed without performing any other searches over the workspace. Specifically, after a global index value is calculated for the reference parameters, comparisons with local indices at *only* a single configuration in the workspace can be overtaken. Hence, searches over workspace is significantly reduced as they are conducted only when it is necessary to calculate new reference global index values. Comparing all set of design variables to find the best worst-case index, the algorithm will converge to an optimum solution within the discretization accuracy. As the culling method substantially reduces the amount of workspace searches required by a brute-force method, it is a fast and efficient algorithm to address min-max type problems.

Since the performance of the culling algorithm is highly dependent on the initial reference values assigned, a fast gradient-based optimization method, sequential quadratic programming (SQP), is used to solve for a local extrema that will serve as a good initialization value. This modification increases the efficiency of the algorithm by resulting in a higher culling rate at the first iteration. Once a solution is obtained, another SQP is invoked to converge to a guaranteed optima within the discretization region.

If the multi-criteria optimization problem is treated as multiple single objective problems where objective functions are handled independently, optimal solution for one criteria may result in an unacceptable design for the other. To achieve a "best" solution with respect to multiple criteria, the trade-off between objectives needs to be quantified. Scalarization approaches assumes apriori knowledge of this trade-off and converts the multi-criteria problem into a single objective one by assigning proper weights or priorities to each performance index. On the other hand, Pareto methods do not require any apriori knowledge about the design trade-offs and solve for the locus of all dominant solutions with respect to multiple objective functions, constituting the so-called the Pareto-front hyper-surface. Hence, designers can make a more realistic choice between multiple "best" solutions and avoid the challenge of synthetically ranking their preferences.

There exists several methods to obtain the Pareto-front hyper-surface, among which Normal Boundary Intersection (NBI) method is one of the most featured. As the Pareto-front hyper-surface is a geometric entity in the objective space forming the boundary of feasible region, NBI approach attacks the *geometric problem* directly by solving for single-objective constrained subproblems to obtain uniformly distributed points on the hyper-surface. NBI solves for subproblems which only depend on the defined optimization model, that is, chosen objective functions and design constraints since these equations map the feasible design space onto the attainable objective space. Given independent optimal solutions for each objective function (solutions of each single objective problem), called shadow points, NBI first constructs an hyper-plane in the objective space by connecting these shadow points with straight lines. Then, this hyper-plane is divided into grids that control the resolution of solutions on the Pareto-front hyper-surface. For each point on the grid, a geometric subproblem is solved to find the *furthest* point on the line that extends along the surface normal passing through the grid point and is in the feasible domain of the objective space. Hence, NBI obtains the Pareto-front with reducing the problem to many single-objective constrained subproblems. Number of subproblems can be adjusted by defining resolution of the grid that maps to the number of points on the Pareto-front hyper-surface. As the number of points increases, the computational time increases linearly, but since the method assumes spatial coherence and uses solution of a subproblem to initialize the next subproblem, convergence time for each subproblem may decrease resulting in further computational efficiency.

NBI methods results in exceptionally uniform distributed points on the Pareto-front hyper-surface without requiring any tuning of the core algorithm. Moreover, once shadow points are obtained, NBI solves for the geometric problem directly utilizing a fast converging gradient-based method, evading the computationally demanding aggregate optimization problems required in for most of the scalarization methods. Therefore, NBI method promises to be much faster and efficient than other methods to obtain a well represented Pareto-front hyper-surface including aggregate methods such as weighted sums and evolutionary optimization approaches such as GAs.

It should also be noted that the NBI method can solve for points on the non-convex regions of Pareto-front hyper-surfaces, a feature that is missing from the weighted sum methods. Compared to weighted sum techniques, NBI achieves higher solution efficiency as it does not suffer from clumping of solution in the objective space. NBI is also advantageous over other methods as it trivially extends to handle any number of objective functions. Compared to Multi-Objective Genetic Algorithm (MOGA) [7] that requires problem dependent fitness and search related tuning and several steps to reach convergence, a standard NBI approach can map the Pareto-front hyper-surface with higher accuracy and uniformity, while also inheriting the efficiency of gradient-based methods.

Relying on gradient techniques, NBI assumes sufficient smooth-

ness of the geometric problem at hand, but it has also been demonstrated that the method performs remarkably well even for non-smooth geometries [27]. In the presence of non-continuous regions, multiple initializations of the NBI method may be required for efficiently generating the Pareto-front hyper-surface. For the case of strongly discontinuous geometries, hybridization with MOGA-II to supply feasible initialization points at each continuous sub-region can be employed, as proposed in [27]. It is noted that since NBI relies on equality constraints, it is possible for NBI not to find a solution on the true Pareto-front hyper-surface, converging to a local optima. In such a case, post processing on the solutions of NBI subproblems can be employed to filter out undesired dominated solutions.

6 Results and Discussion

Table 2 presents the results of the modified culling algorithm for the single objective problems, for best kinematic and dynamic isotropy, respectively. These results are obtained conducting a global search over the entire parameter space with discretization step sizes of 2mm and 1mm for the parameter and workspace, respectively, and performs several local searches with finer discretizations at the neighborhood of the results suggested by the global search.

Table 2: Results of independent optimizations with respect to $\mathcal{GII}$ and $\mathcal{GDI}$.

	Best Design for Kinematic Isotropy	**Best Design for Dynamic Isotropy**	**Unit**
$\mathcal{GII}$	0.783	0.407	–
$\mathcal{GDI}$	0.622	0.766	–
l_0	0.4	0.1	mm
l_1	299.7	89.9	mm
l_2	300.0	115.2	mm
r	419.6	123.6	mm

Figure 2 presents the change of singular values over the workspace for the optima of single objective problems. Subfigures 2(a) and 2(c) pertain to the best kinematic design while Subfigures 2(b) and 2(d) belong to best dynamic design. Results indicate that best design with respect to solely $\mathcal{GII}$ suffers from poor dynamic performance, while best design with respect to only $\mathcal{GDI}$ possesses poor kinematic performance.

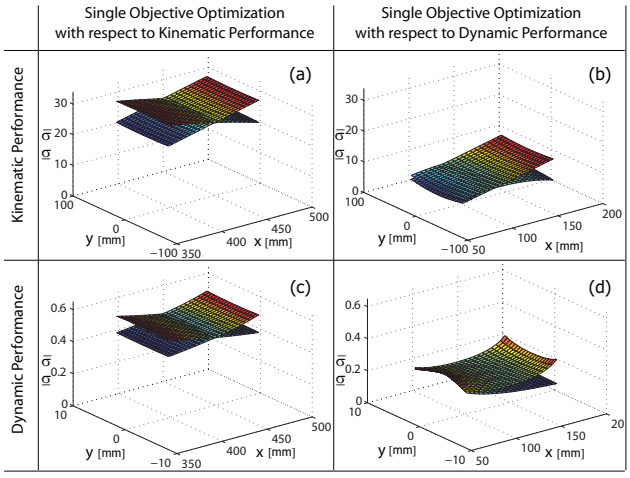

Figure 2: Change of singular values over the workspace for the optima of single objective problems. Subfigures (a) and (c) pertain to the best kinematic design, while (b) and (d) belong to the best dynamic design.

To characterize the trade-off between the single objective solutions, Pareto-front curve for the bi-objective optimization problem is constructed in Figure 3. Two different techniques are employed to form the Pareto-front curve, namely NBI method and aggregated performance index method. For the NBI method, a grid size of ten points are selected. In Figure 3 the distribution of points on the Pareto-front curve is marked by dots. For the second method, an aggregated performance index ($\mathcal{API}$) is defined as the weighted linear combination of $\mathcal{GII}$ and $\mathcal{GDI}$. In particular, $\mathcal{API} = \lambda\,\mathcal{GII} + (1-\lambda)\,\mathcal{GDI}$, where $0 \leq \lambda \leq 1$ denotes the weighting factor. Ten aggregated optimization problems are solved for ten equally spaced weighting factors utilizing the modified culling algorithm with discretization step sizes of 5mm for the parameter space and 1mm for the workspace. Circles in the Figure 3 denote the distribution of aggregate solutions on the Pareto-front curve and are marked with their corresponding weighting factor.

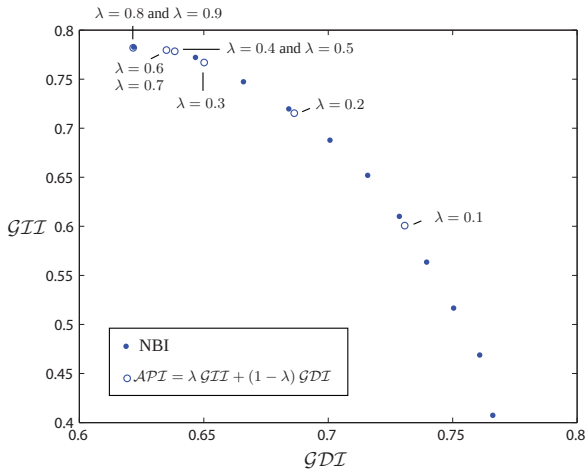

Figure 3: Comparison of NBI and aggregated performance index methods. Symbol λ is the weighting factor.

As expected, NBI method generates a very uniform distribution of points on the Pareto-front curve while the solutions of the aggregate problem are clumped at certain locations of the curve. To obtain a uniform distribution using the aggregated index approach, proper weights should be assigned to ensure uniform distribution. However, the characteristics of the weight distribution is not known before the problem is solved. Moreover, since the aggregate performance index relies on the relatively costly culling algorithm to solve for each point on the Pareto-front curve, its accuracy is limited by the discretization step size chosen. In the Figure 3, the same solutions are obtained for different weighting factors, particulary for weighting factors $\lambda = 0.4$ to $\lambda = 0.5$, $\lambda = 0.6$ to $\lambda = 0.7$, and $\lambda = 0.8$ to $\lambda = 0.9$, respectively, due to the course discretization used. Unfortunately, solving for each aggregate performance index at each weighting is a computationally demanding task, limiting the density of feasible discretization. NBI method possesses an inherent advantage in terms of computational cost, as it attacks the direct geometric problem to obtain the Pareto-front curve and utilizes continuous, computationally efficient gradient methods for the solution.

In addition to the efficiency offered via the uniform distribution of solutions on the Pareto-front curve, NBI approach results in *orders of magnitude* improvement in the computation time, especially for the design problem at hand, as depicted in Figure 4. All of the simulations presented in Figure 4 are performed using a 32 bit Windows XP workstation that is equipped with a 3.40GHz Intel Xeon processor with 1MB L2 cache and 4GB DDR-2 400MHz SDRAM.

As can be observed from Figure 4, the aggregate problem scales geometrically with the discretization step size, rendering an accurate solution of even ten points on the Pareto-curve almost impossible for the simple sample problem at hand. On the other hand,

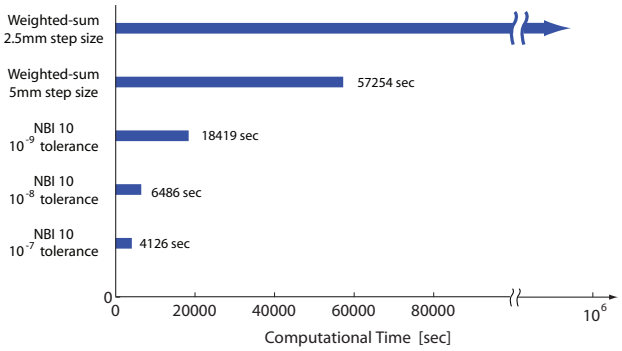

Figure 4: Computational effort of NBI method with respect to different tolerances and weighted sum method with respect to different discretizations.

NBI method solves for points on the Pareto-front curve very effectively, in about 1/3 time of the weighted-sum approach with 5mm step size. Even though the accuracy of solutions obtained by the NBI method is dependent on the constraint tolerance set for the algorithm, convergence for NBI with all reasonable tolerance values are shown to be acceptable in Figure 5. Particularly, Figure 5 presents solutions obtained using the NBI approach with three different tolerance values: 10^{-7}, 10^{-8}, and 10^{-9}. Since NBI employs a local search algorithm that is dependent on the initial conditions, convergence can be poor at certain trials as can be observed for two points in Figure 5. However, poor convergence of certain points is not an uncorrectable drawback, as solution for those points can be repeated with different initializations and tighter tolerances. The computational time for NBI method scales linearly with tolerance values as it does with number of points selected for the grid.

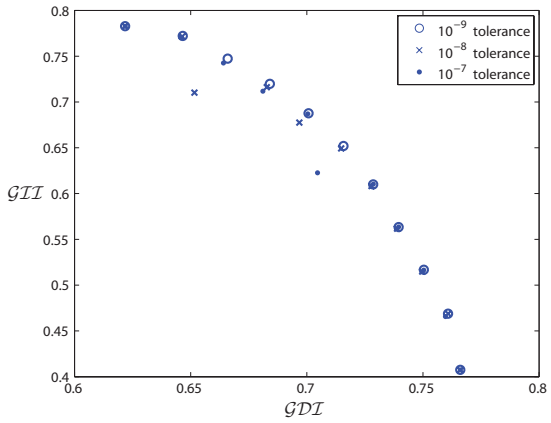

Figure 5: Distribution NBI solutions with three different tolerances: 10^{-7}, 10^{-8}, and 10^{-9}.

To allow for further comparisons of the Pareto methods with other scalarization approaches proposed in the literature, a sequential optimization is implemented for the sample problem as suggested in [32]. In this method, firstly parameter sets resulting in the best $\mathcal{GII}$ values for each discrete value of the parameter r are calculated using the culling algorithm. The change in $\mathcal{GII}$ values and the link lengths are plotted in Figure 6 with respect to the independent parameter r. In this plot, one can observe that $\mathcal{GII}$ value increases monotonically with increasing r until the link length l_1 reaches its allowable upper limit (300mm) while link lengths l_0 and l_2 also increase with increasing r until l_2 reaches its allowable upper limit (300mm). Once l_2 reaches its upper limit, monotonic decrease in l_0 values can be observed until l_1 reaches its upper limit.

Assigning r as the independent variable, the sequential method

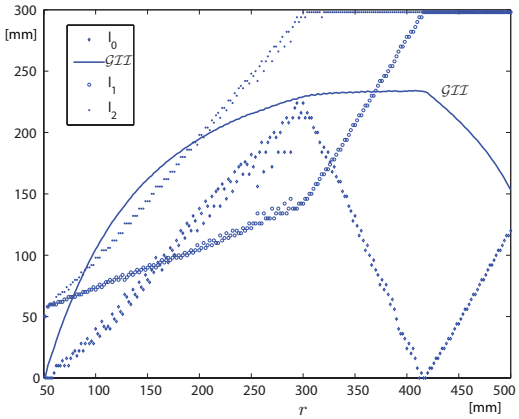

Figure 6: The parameter sets with best $\mathcal{GII}$ values for each discrete value of r.

uses the set of "optimal" solutions with respect to $\mathcal{GII}$ as the feasible search domain to conduct another single criteria optimization, this time with respect to $\mathcal{GDI}$. In other words, the parameter set resulting in the best $\mathcal{GDI}$ value is selected from the Figure 6, utilizing the culling algorithm. The result of the sequential optimization approach is plotted in Figure 7 with respect to a dense Pareto-curve obtained using the NBI approach. Inspecting the plot, one can conclude that the "best" solution obtained using the sequential optimization approach is *dominated* – is a point not lying on the pareto front, meaning there exists solutions for which one can improve $\mathcal{GII}$ while keeping $\mathcal{GDI}$ constant or vice versa. In fact, improvements up to 20% in the $\mathcal{GII}$ value and up to 3% in the $\mathcal{GDI}$ value are possible by choosing one of the designs that lies on the Pareto-front boundary found by the intersection of the Pareto curve and vertical and horizontal line, respectively, passing through that point.

As emphasized earlier, any point on the Pareto-front curve is a non-dominated solution. Hence it is up to the designer to chose the "best" design for the application at hand, considering the characteristic of the trade-off mapped out by the Pareto-front boundary. The Pareto methods not only allow additional constraints be considered for the final decision but also let the designer adjust these constraints while simultaneously monitoring their effect on the set of non-dominated solutions. For the sample problem analyzed, a design is selected by imposing two additional physical constraints on the Pareto-front curve: a limit on the allowable workspace and a limit on the actuator size. Assuming that DC motors with 40mm diameter (Maxon RE40) will be used as the actuators, a new lower limit can be imposed on the link lengths as $l_0 > 40$mm, rendering the last 11 points on the Pareto-front curve as infeasible designs. As for the second constraint, the footprint of the mechanism is to be restricted. The designer can impose constraints of different footprint areas to observe their effect on the non-dominated solution set. In Figure 7 infeasible solutions for footprint areas of 300mm x 300mm and 400mm x 400mm are marked. Noticing that there are still feasible solutions on the current Pareto-front curve for a footprint area of 300mm x 300mm, a design is selected to satisfy both of these constraints as marked by the star in Figure 7. The link lengths corresponding to this design choice is also represented in Figure 7.

7 Conclusions and Future Work

A general framework suitable for optimization of haptic interfaces, in particular haptic interfaces with closed kinematic chains, with respect to the multiple design criteria is presented. Optimization problems for haptic interfaces with best worst-case kinematic and dynamic performance are formulated. Non-convex single objective optimization problems are solved with the modified culling algo-

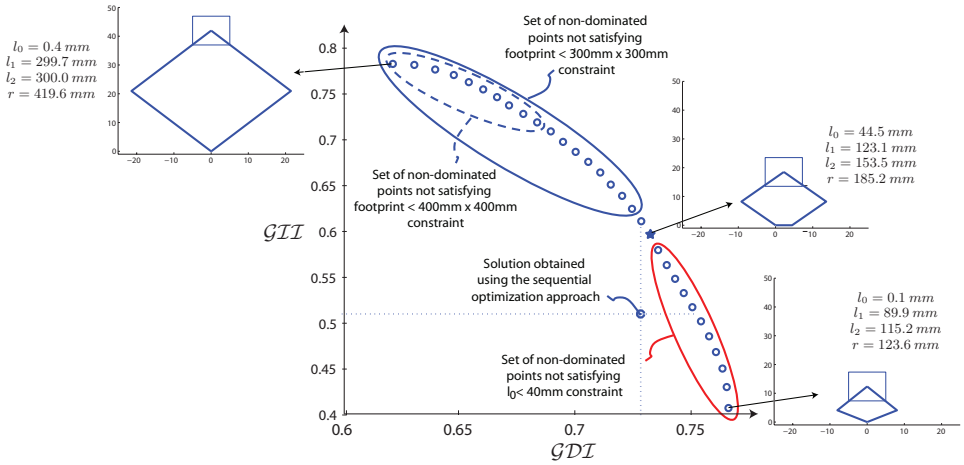

Figure 7: Comparison of sequential approach with the Pareto-front curve. Effects of additional constraints imposed on the problem and link lengths corresponding to "best" designs.

rithm, while NBI method is used to obtain the Pareto-front curve to present the designer with a wide range of alternative solutions. Computational efficiency of NBI method is demonstrated over aggregating approaches such as weighted sums. The optimality of the design using Pareto methods is shown over prioritization approaches. Dimensional synthesis of a high performance haptic interface utilizing the Pareto-front curve is demonstrated.

The method is extensible to work with various performance indices and to include any number of criteria. Application of the proposed framework to the design of more complex haptic interfaces incorporating increased number of multi-objectives and their solution via hybrid techniques will be addressed in the future.

Acknowledgements

The authors gratefully acknowledge Aimin Zhou for his contributions during implementation of NBI method and the scholarship provided by Sabancı Univerity, Faculty of Engineering and Natural Sciences.

References

[1] G. Alici and B. Shirinzadeh. Optimum synthesis of planar parallel manipulators based on kinematic isotropy and force balancing. *Robotica*, 22(1):97–108, 2004.

[2] H. Asada. A geometrical representation of manipulator dynamics and its application to arm design. *ASME Journal of Dynamic Systems, Measurement, and Control*, 105(3):131–135, 1983.

[3] W. Chen, Q. Zhang, Z. Zhao, and W. A. Gruver. Optimizing multiple performance criteria in redundant manipulators by subtask-priority control. In *IEEE International Conference on Systems, Man and Cybernetics*, volume 3, pages 2534–2539, 1995.

[4] C. A. Coello. An updated survey of GA-based multiobjective optimization techniques. *ACM Computing Surveys*, 32(2):109–143, 2000.

[5] I. Das and J. E. Dennis. Normal-boundary intersection: A new method for generating the pareto surface in nonlinear multi-criteria optimization problems. *SIAM Journal on Optimization*, 8(3):631–65, 1996.

[6] O. L. de Weck. Multiobjective optimization: History and promise. In *China-Japan-Korea Joint Symposium on Optimization of Structural and Mechanical Systems*, Invited Keynote Paper, 2004.

[7] C. M. Fonseca and P. J. Fleming. Genetic algorithms for multiobjective optimization: Formulation, discussion and generalization. In *Multiobjective evolutionary algorithms: Empirical Genetic Algorithms*, pages 416–423, 1993.

[8] C. Gosselin and J. Angeles. A global performance index for the kinematic optimization of robotic manipulators. *ASME Journal of Mechanical Design*, 113(3):220–226, 1991.

[9] K. Grace and J. Colgate. A six degree-of freedom micromanipulator for ophthalmic surgery. In *IEEE International Conference on Robotics and Automation*, volume 1, pages 630–635, 1993.

[10] R. D. Gregorio and V. Parenti-Castelli. On the characterization of the dynamic performances of planar manipulators. *Meccanica*, 40(3):267–279, 2005.

[11] V. Hayward, J. Choksi, G. Lanvin, and C. Ramstein. Design and multiobjective optimization of a linkage for a haptic interface. In *Advances in Robot Kinematics*, pages 352–359, 1994.

[12] H. Ishibuchi and K. Narukawa. Comparison of evolutionary multiobjective optimization with reference solution-based single-objective approach. In *Genetic and Evolutionary Computation*, pages 787–794, 2005.

[13] W. A. Khan and J. Angeles. The kinetostatic optimization of robotic manipulators: The inverse and the direct problems. *Transaction of ASME Journal of Mechanical Design*, 128(1):168–178, 2006.

[14] C. A. Klein and B. E. Blaho. Dexterity measures for the design and control of kinematically redundant manipulators. *The International Journal of Robotics Research*, 4(2):72–83, 1987.

[15] M. Krefft and J. Hesselbach. Elastodynamic optimization of parallel kinematics. In *IEEE International Conference on Automation Science and Engineering*, pages 357–362, 2005.

[16] M. Krefft and J. Hesselbach. Elastodynamic optimization of parallel kinematics. In *IEEE International Conference on Automation Science and Engineering*, pages 357–362, 2005.

[17] M. Krefft, H. Kerle, and J. Hesselbach. The assesment of parallel mechanisms – it is not only kinematics. *Production Engineering*, 12(1):173–173, 2005.

[18] J. H. Lee, K. S. Eom, B.-J. Yi, and I. H. Suh. Design of a new 6-DoF parallel haptic device. In *IEEE International Conference on Robotics and Automation*, volume 1, pages 886–891, 2001.

[19] S.-U. Lee and S. Kim. Analysis and optimal design of a new 6-DoF parallel type haptic device. In *IEEE/RSJ International Conference on Intelligent Robots and Systems*, pages 460–465, 2006.

[20] X.-J. Liu and J. Wang. A new methodology for optimal kinematic design of parallel mechanisms. *Mechanism and Machine Theory*, 42:1210–1224, 2007.

[21] X.-J. Liu, J. Wang, and H.-J. Zheng. Optimum design of the 5R symmetrical parallel manipulator with a surrounded and good-condition workspace. *Robotics and Autonomous Systems*, 54(3):221–233, 2006.

[22] Y. Lou, G. Liu, and Z. Li. Randomized optimal design of parallel manipulators. *IEEE Transactions on Automation Science and Engineering*, to appear.

[23] O. Ma and J. Angeles. The concept of dynamic isotropy and its applications to inverse kinematics and trajectory planning. In *IEEE International Conference on Robotics and Automation*, volume 1, pages 481–486, 1990.

[24] S. McGhee, T. F. Chan, R. V. Dubey, and R. L. Kress. Probability-

based weighting of performance criteria for a redundant manipulator. In *ICRA*, pages 1887–1894, 1994.

[25] H. Ozaki, H. Wang, X. Liu, and F. Gao. The atlas of the payload capability for design of 2-DoF planar parallel manipulators. In *IEEE International Conference on Systems, Man, and Cybernetics*, volume 2, pages 1483–1488, 1996.

[26] L. Qi and R. S. Womersley. On extreme singular values of matrix valued functions. *Journal of Convex Analysis*, 3(1):153–166, 1996.

[27] E. Rigoni and S. Poles. NBI and MOGA-II, two complementary algorithms for multi-objective optimizations. In *Practical Approaches to Multi-Objective Optimization*, 2005.

[28] A. Risoli, G. M. Prisco, F. Salsedo, and M. Bergamasco. A two degrees-of-freedom planar haptic interface with high kinematic isotropy. In *IEEE International Workshop on Robot and Human Interaction*, pages 297–302, 1999.

[29] J. K. Salisbury and J. J. Craig. Articulated hands: Force control and kinematic issues. *The International Journal of Robotics Research*, 1(1):4–17, 1982.

[30] S.-D. Stan, V. Maties, and R. Balan. Optimal design of 2 DoF parallel kinematics machines. In *Applied Mathematics and Mechanics*, pages 705–706, 2006.

[31] L. Stocco, S. E. Salcudean, and F. Sassani. Fast constrained global minimax optimization of robot parameters. *Robotica*, 16(6):595–605, 1998.

[32] L. J. Stocco. *Robot design optimization with haptic interface applications*. PhD thesis, The University of British Columbia, 1999.

[33] B. Stuckman and E. Easom. A comparison of bayesian/sampling global optimization techniques. *IEEE Transactions of Systems, Man and Cybernetics*, 22(5):1024–1032, 1992.

[34] B. Stuckman, G. Evans, and M. Mollaghasemi. Comparison of global search methods for design optimization using simulation. In *IEEE Winter Simulation Conference*, pages 937–944, 1991.

[35] J. Yoon and J. Ryu. Design, fabrication, and evaluation of a new haptic device using a parallel mechanism. *IEEE/ASME Transactions on Mechatronics*, 6(3):221–233, 2001.

[36] T. Yoshikawa. Dynamic manipulability of robotic mechanisms. *Journal of Robotic Systems*, 2(1):113–123, 1985.

[37] T. Yoshikawa. Manipulability of robotic mechanisms. *The International Journal of Robotics Research*, 4(2):3–9, 1985.

[38] Y. Zheng and W. Lewis. Several algorithms of global optimal search. *Advances in Enginering Software*, 22(2):87–98, 1994.

APPENDIX

The aim of this appendix is to provide the necessary steps for derivation of the Jacobian and mass matrices of a symmetric five-bar mechanism. To set the notation, let a symbol in standard typeface represent the norm or length of the corresponding vector marked by an arrow.

The Jacobian matrix of the mechanism is required to determine its kinematics performance. To construct the Jacobian, the end-effector velocities are to be expressed in terms of the angular velocities of the actuators through a forward kinematics analysis. Let each rigid link of the mechanism be defined as a body and assign a vector basis to each body with the first basis vector extending along the link length. Bodies A, B, C, and D along with their vector bases are shown in Figure 8. The end-effector point is denoted by E while symbol N is used to signify the Newtonian reference frame. Point O represents a fixed point that is selected as the origin.

Symbols x and y denote the end-effector positions in the Newtonian frame N, while the distance between actuators and the link lengths are called l_0 and l_i ($i = 1..4$), respectively. Finally, the orientation of the links are measured with respect to the basis vector $\vec{n}_1$ and are called q_i ($i = 1..4$). Note that the mechanism is assumed to be symmetric; hence, the equalities $l_2 = l_3$, $l_1 = l_4$ are in effect.

The vector loop equation enforcing the closed kinematic chain for the symmetric five bar mechanism can be formulated as

$$l_1\vec{a}_1 + l_2\vec{b}_1 - l_2\vec{c}_1 - l_1\vec{d}_1 - l_0\vec{n}_1 = \vec{0}. \tag{4}$$

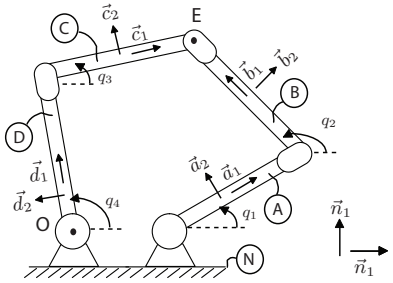

Figure 8: Symmetric five-bar mechanism with the variables used in the kinematic and dynamic analyses.

Taking time derivative of Eqn. (4) in the Newtonian frame, one can solve for the time derivatives of dependent variables q_2 and q_3, in terms of the angular speeds of the actuators $\dot{q}_1$ and $\dot{q}_4$ as

$$\begin{bmatrix} \dot{q}_2 \\ \dot{q}_3 \end{bmatrix} = A \begin{bmatrix} \dot{q}_1 \\ \dot{q}_4 \end{bmatrix} \tag{5}$$

where $A = \begin{bmatrix} \frac{-l_1\sin(q_1-q_3)}{l_2\sin(q_2-q_3)} & \frac{-l_1\sin(q_3-q_4)}{l_2\sin(q_2-q_3)} \\ \frac{-l_1\sin(q_1-q_2)}{l_2\sin(q_2-q_3)} & \frac{-l_1\sin(q_2-q_4)}{l_2\sin(q_2-q_3)} \end{bmatrix}$.

The position of the end-effector E with respect to the fixed point O can be expressed as

$$\vec{p}^{\,OE} = l_1\vec{a}_1 + l_2\vec{a}_2 \tag{6}$$

while the same position vector can also be expressed in the Newtonian frame as

$$\vec{p}^{\,OE} = x\vec{n}_1 + y\vec{n}_2. \tag{7}$$

Equating Eqn. (6) to Eqn. (7), taking their time derivative in the Newtonian frame, and substituting in Eqn. (5), one can solve for the velocity level forward kinematics of the five-bar mechanism as

$$\begin{bmatrix} \dot{x} \\ \dot{y} \end{bmatrix} = J \begin{bmatrix} \dot{q}_1 \\ \dot{q}_4 \end{bmatrix} \tag{8}$$

where the Jacobian matrix

$$J = \begin{bmatrix} \frac{-l_1\sin(q_1)-\sin(q_2)\sin(q_1-q_3)}{\sin(q_2-q_3)} & \frac{l_1\sin(q_2)\sin(q_3-q_4)}{\sin(q_2-q_3)} \\ \frac{l_1\cos(q_1)-\cos(q_2)\sin(q_1-q_3)}{\sin(q_2-q_3)} & \frac{-l_1\cos(q_2)\sin(q_3-q_4)}{\sin(q_2-q_3)} \end{bmatrix}.$$

To solve for the effective mass matrix of the system as seen at the end-effector, dynamic analysis is performed employing Lagrange's method. The kinetic co-energy $\mathcal{T}^*$ of the five-bar linkage is calculated as

$$\begin{aligned} \mathcal{T}^* = {} & \tfrac{1}{24}m_1(k^2+4l_1^2)\dot{q}_1^2 + \tfrac{1}{24}(3m_1l_1^2 + m_4(k^2+l_1^2))\dot{q}_4^2 \\ & + \tfrac{1}{24}m_2(k^2\dot{q}_2^2 + 4l_2^2\dot{q}_2^2 + 12l_1^2\dot{q}_1^2 + 12l_1l_2\cos(q_1-q_2)\dot{q}_1\dot{q}_2) \\ & + \tfrac{1}{24}m_3(k^2\dot{q}_3^2 + 4l_2^2\dot{q}_3^2 + 12l_1^2\dot{q}_4^2 + 12l_1l_2\cos(q_3-q_4)\dot{q}_3\dot{q}_4) \end{aligned} \tag{9}$$

Since the gravity acts out of the plane of the mechanism, the kinetic co-energy of the system is equal to the Lagrangian $\mathcal{L}$ of the system. Invoking Lagrange's equation, the elements of the mass matrix D can be derived as

$D_{11} = \frac{1}{12}m_1(k^2+4l_1^2) + \frac{1}{12}m_3l_1^2\sin(q_1-q_2)^2(4/\sin(q_2-q_3)^2 + k^2/l_2^2/\sin(q_2-q_3)^2) + \frac{1}{12}m_2l_1^2(12 + k^2\sin(q_1-q_3)^2/l_2^2/\sin(q_2-q_3)^2 + 4\sin(q_1-q_3)(\sin(q_1-q_3) - 3\sin(q_2-q_3)\cos(q_1-q_2))/\sin(q_2-q_3)^2)$

$D_{12} = \frac{1}{12}l_1^2(m_2\sin(q_3-q_4)(k^2\sin(q_1-q_3)/l_2^2/\sin(q_2-q_3)^2 + (4\sin(q_1-q_3) - 6\sin(q_2-q_3)\cos(q_1-q_2))/\sin(q_2-q_3)^2) + m_3\sin(q_1-q_2)(k^2\sin(q_2-q_4)/l_2^2/\sin(q_2-q_3)^2 + (4\sin(q_2-q_4) - 6\sin(q_2-q_3)\cos(q_3-q_4))/\sin(q_2-q_3)^2))$

$D_{22} = \frac{1}{4}m_1l_1^2 + \frac{1}{12}m_4(k^2+l_1^2) + \frac{1}{12}m_2l_1^2\sin(q_3-q_4)^2(4/\sin(q_2-q_3)^2 + k^2/l_2^2/\sin(q_2-q_3)^2) + \frac{1}{12}m_3l_1^2(12 + k^2\sin(q_2-q_4)^2/l_2^2/\sin(q_2-q_3)^2 + 4\sin(q_2-q_4)(\sin(q_2-q_4) - 3\sin(q_2-q_3)\cos(q_3-q_4))/\sin(q_2-q_3)^2)$.

Finally, the effective mass matrix of the system as seen at the end-effector can then be calculated using

$$M = J^{-T}\, D\, J^{-1}. \tag{10}$$